

Optical/IR studies of Be stars in NGC 6834 with emphasis on two specific stars

Blesson Mathew^{1,4}, Watson P. Varricatt², Annapurni Subramaniam³, N. M. Ashok⁴ and D. P. K. Banerjee⁴

¹ Centre for Astrophysics & Supercomputing, Swinburne University, Hawthorn VIC 3122, Australia; blessonmathew@gmail.com

² Joint Astronomy Centre, 660 N. Aohoku Pl., Hilo, HI 96720, USA

³ Indian Institute of Astrophysics, Bangalore - 560 034, India

⁴ Astronomy and Astrophysics Division, Physical Research Laboratory, Navrangapura, Ahmedabad - 380 009, Gujarat, India

Received 2014 February 12; accepted 2014 March 24

Abstract We present optical and infrared photometric and spectroscopic studies of two Be stars in the 70–80-Myr-old open cluster NGC 6834. NGC 6834(1) has been reported as a binary from speckle interferometric studies whereas NGC 6834(2) may possibly be a γ Cas-like variable. Infrared photometry and spectroscopy from the United Kingdom Infrared Telescope (UKIRT), and optical data from various facilities are combined with archival data to understand the nature of these candidates. High signal-to-noise near-IR spectra obtained from UKIRT have enabled us to study the optical depth effects in the hydrogen emission lines of these stars. We have explored the spectral classification scheme based on the intensity of emission lines in the H and K bands and contrasted it with the conventional classification based on the intensity of hydrogen and helium absorption lines. This work also presents hitherto unavailable UBV CCD photometry of NGC 6834, from which the evolutionary state of the Be stars is identified.

Key words: stars: emission-line, Be — circumstellar matter — infrared: stars — line: profiles — (Galaxy:) open clusters and associations: individual (NGC 6834)

1 INTRODUCTION

Classical Be stars are non-supergiant B-type stars that show, or have shown, Balmer emission lines in their spectra at least once in their lifetime (Collins 1987; Porter & Rivinius 2003). These, and other recombination lines of hydrogen, are formed in a circumstellar disk that is formed through the decretion mechanism (see Rivinius et al. 2013 for a recent review). Be stars rotate close to the critical velocity (Townsend et al. 2004). This, along with non-radial pulsations, assists the formation of the disk (also known as the ‘Be phenomenon,’ Slettebak 1988). Although recent theoretical models such as the viscous decretion disk model explain the formation of the disk once the mass is accumulated in the circumstellar medium, the mode of mass transfer from the star to the disk is still an open issue. This problem can be resolved from the study of a large sample of Be stars in diverse

environments, such as in the galactic field and in open clusters. The near-infrared spectral region is ideally suited for studies of this kind since the extinction is much lower (only \sim one-tenth that of optical in the K band) and ‘IR excess’ starts showing up in the JHK bands (Dougherty et al. 1994). From the pioneering study of Gehrz et al. (1974), it is understood that the disk contributes excess flux in the infrared, which appears as IR excess over the stellar photospheric continuum. The IR excess has been quantified by means of free-free and free-bound emission from the electrons in the gaseous disk without an additional contribution from dust (Ashok et al. 1984; Banerjee et al. 2001). In addition to continuum emission, the H I recombination lines formed in the disk fill up the photospheric absorption profiles and appear as emission lines. The H I recombination lines are subjected to opacity effects, which suggest that the line formation region in the disk is extremely dense, with an electron density of $10^{10} - 10^{14} \text{ cm}^{-3}$ (Mathew et al. 2012b; Ashok & Banerjee 2000). Clark & Steele (2000) were the first to conduct a systematic study on the spectra of Be stars in the K band, which was followed by a similar study in the H band by Steele & Clark (2001). They proposed a scheme to identify the spectral types of Be stars from the intensity of emission lines in the H and K bands, which is a promising method to classify highly reddened Be stars that are counterparts of X-ray transient systems.

To gain a better understanding of the Be phenomenon it is necessary to study the infrared spectra of Be stars in diverse environments. All of the previous spectroscopic studies of Be stars, especially in the infrared, have concentrated on nearby field stars. The prime reason is that they are within a distance of 1 kpc, which makes them bright enough to be observed even with 1-m class telescopes. This paper presents the first of our efforts to study the infrared spectra of Be stars in young (< 100 Myr) open clusters, at distances greater than 1 kpc. In this work we present infrared spectroscopy of two Be stars associated with the cluster NGC 6834, located at a distance of 3.1 kpc.

NGC 6834 is a young open cluster in Cygnus, belonging to the Trumpler type II 2 m (II - detached cluster with a little central concentration, 2 - moderate range in brightness, m - medium rich (50–100 stars), Ruprecht 1966). A range of distance estimates are available for this cluster - from 2100 pc reported by Fünfschilling (1967) to 2750 pc from the studies of Miller et al. (1996). Paunzen et al. (2006) estimated a distance of 1930 ± 32 pc from CCD observations in the g_1g_2y photometric system, which matches the earlier estimates by Trumpler (1930). Similarly, one can find diverse age estimates; Miller et al. (1996) estimated the age of the cluster to be around 50 Myr, while Moffat (1972) assigned a value of 80 Myr. Paunzen et al. (2006) estimated a mean color excess $E(B - V) = 0.70 \pm 0.05$ mag, and Jerzykiewicz et al. (2011) found a range in $E(B - V)$ values between 0.61 and 0.82 mag. Jerzykiewicz et al. (2011) identified 15 B-type variable stars in the cluster. They found five cluster members showing H α emission, including a γ Cas-type variable and two λ Eri-type variables. Miller et al. (1996) found six Be stars in the cluster from broadband photometry and observations using narrow-band filters centered on the H α line and the adjacent continuum. Mathew et al. (2008), in their slitless spectroscopic survey to identify emission-line stars in young Galactic open clusters, identified four Be stars in this cluster. The Be stars showing faint H α emission that barely fills up the absorption profile and remains below the continuum level will not be detected through slitless spectroscopy. Hence, there could be many more Be stars in the cluster, as reported by Miller et al. (1996) and Jerzykiewicz et al. (2011). However, since these detections were based on narrow-band H α photometry, the Be status has to be confirmed through spectroscopy and until this is done we assume that there are only four Be stars in NGC 6834, whose spectral analysis has been done and whose Be status has been confirmed (Mathew & Subramaniam 2011).

The Be stars were cataloged as NGC 6834(1), NGC 6834(2), NGC 6834(3) and NGC 6834(4) in Mathew & Subramaniam (2011), while their corresponding numbers in WEBDA are 55, 67, 106 and 36 (based on the numbering scheme of Fünfschilling 1967). Jerzykiewicz et al. (2011) identified the stars 55 and 67 (named by them V6 and V2 respectively) as variables, with the latter classified as a γ Cas-like variable. Among the four Be stars, NGC 6834(1) and NGC 6834(2) show a high value of H α equivalent width (EW) ($\sim 40 \text{ \AA}$), which is also a reasonably high value among the sample

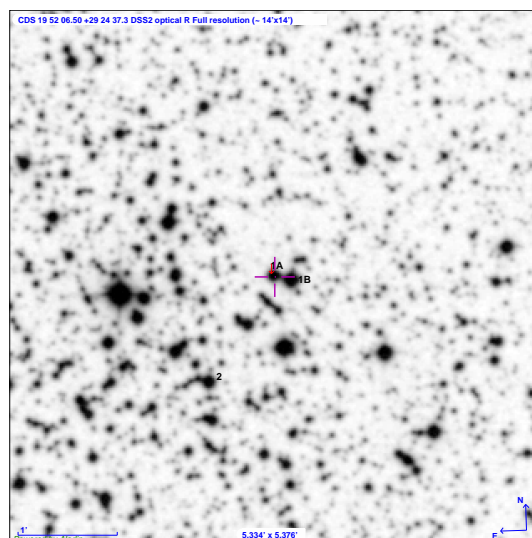


Fig. 1 The Be stars NGC 6834(1) and NGC 6834(2) are shown in the POSS II plate, labeled 1A and 2, respectively. Also shown is the possible companion to NGC 6834(1), reported by Mason et al. (2002), as 1B.

of classical Be stars in open clusters (Mathew & Subramaniam 2011). The intense $H\alpha$ emission in these two candidates is supported from the studies of Jerzykiewicz et al. (2011), who quantified it by means of the α index ($H\alpha_{\text{line}} - H\alpha_{\text{continuum}}$). The Be stars NGC 6834(1) and NGC 6834(2) are shown in Figure 1.

The motivations for the present study are summarized as follows:

- (1) Previous infrared spectroscopic studies of Be stars have concentrated on bright, nearby field Be stars. To the best of our knowledge, this is the first effort to study Be stars that are members of young (<100 Myr), distant (>1 kpc) open clusters. More studies are planned in this direction, which will address the role of the cluster environment in the formation of a disk in Be stars. Most of the Be stars, which are members of open clusters and were identified in the survey by Mathew et al. (2008); Mathew & Subramaniam (2011) are at a distance greater than 3 kpc; these sources can be studied in the infrared using facilities with capacity similar to that of UKIRT. The IR spectroscopy when combined with optical spectra and available archival data (in a similar fashion as we have done in this work) will provide insights about the nature of the circumstellar disk in Be stars.
- (2) A recombination analysis of the flux ratios of emission lines belonging to Brackett and Pfund series of hydrogen, as well as a comparison with the theoretical estimates, addresses the role of optical depth effects in these systems. In the future, we plan to use optical spectra covering Balmer and higher order Paschen lines, in conjunction with infrared spectra, which will enable us to perform elaborate recombination line analysis over optical and infrared bands.
- (3) The stars NGC 6834(1) and NGC 6834(2) are selected for this study due to the following reasons: (i) Mason et al. (2002) identified a possible companion to NGC 6834(1) at a distance of $10.35''$ from speckle interferometric studies (shown as 1B in Fig. 1); (ii) NGC 6834(2) has been found to exhibit long-term and short-term variability and, based on the short-term variability and the presence of $H\alpha$ emission, Jerzykiewicz et al. (2011) classified this star as a γ Cas-like vari-

able; and, (iii) both stars are found to exhibit strong $H\alpha$ emission, which suggests the possible presence of an extended circumstellar disk.

- (4) There is an uncertainty about the spectral types of these stars (in Sect. 3.3 we re-assess their spectral types from optical and infrared spectroscopy). In addition, a clear picture of the evolutionary status of these stars can be obtained from the optical color-magnitude diagram, which is constructed using the newly obtained photometric data.

The paper is arranged as follows. Section 2 elaborates on the optical and infrared data used in this work. The results of this study are presented in Section 3. Based on the available observations, the nature of the two Be stars is discussed in Section 4.

2 OBSERVATIONS AND ANALYSIS

Near-infrared photometric and spectroscopic observations of the target stars were obtained. These data are combined with new optical photometric and spectroscopic data, and archival optical and IR data to gain a better understanding of the objects under study. The details of the observations and data analysis are given below.

2.1 Near-Infrared Spectroscopy

Observations were carried out with the 3.8-m United Kingdom Infrared Telescope (UKIRT), Hawaii, using the UKIRT Imager-Spectrometer (UIST; Ramsay Howat et al. 2004). A 4-pixel-wide slit ($0.46''$) was used, which gives a spectral resolving power of 550 when observed with the HK grism, and 1500 with the short- J grism. The observations were performed by alternating the object between two positions separated by $12''$ along the slit. A black body unit mounted on the instrument was used for flat fielding. Arc spectra obtained with an argon lamp were used for wavelength calibration. Preliminary data reduction (including flat fielding, subtracting the dithered frames and coadding these subtracted pairs) was carried out using the UKIRT pipeline ORACDR. The final extraction of the spectra, wavelength calibration, ratioing and flux calibration were done using the STARLINK packages FIGARO and KAPPA, and the NOAO package Image Reduction and Analysis Facility (IRAF).

To remove the telluric absorption bands from the object spectra, BS 7793 (HD 194012; F8V) was observed immediately before the object, at a similar airmass. We used the NASA Infrared Telescope Facility (IRTF) spectrum of HD 219623 (Rayner et al. 2009), which has a similar spectral type, taken from the NASA IRTF spectral library, to derive the sky and the instrument transmission function. The IRTF spectrum of HD 219623, which has a higher spectral resolution, was smoothed to match the resolution of the object spectra and was then interpolated between 18050 and 19300 Å where the sky transmission is poor. The wavelength calibrated spectrum of BS 7793 was then divided by the modified IRTF spectrum to remove the slope of the stellar spectral energy distribution (SED) and the photospheric absorption lines. The extracted, wavelength calibrated object spectra were then divided by the ratioed spectrum. The HK spectra were normalized at the central wavelength of the K -band, and were then multiplied by the 2MASS K -band flux values to flux calibrate the object spectra. The short- J spectra were not flux calibrated since the central wavelength of the J band filter falls outside the wavelength range covered by the short- J grism. The log of the observations is given in Table 1.

2.2 Infrared Photometry

2.2.1 JHK photometry

The JHK photometry was performed with the UKIRT Fast-Track Imager (UFTI; Roche et al. 2003) mounted on UKIRT. Observations were carried out in photometric sky conditions (see Table 2 for

Table 1 Journal of infrared spectroscopic observations from UKIRT. Observations were done on 2006–10–23.

Object	Grism	UT	Mean airmass	Integration time (s)
NGC 6834(1)	<i>HK</i>	06:25:39	1.19	720
NGC 6834(2)	<i>HK</i>	06:42:35	1.24	480
NGC 6834(1)	short- <i>J</i>	07:08:10	1.35	1440
NGC 6834(2)	short- <i>J</i>	07:29:39	1.46	720

Table 2 Journal of infrared photometric observations from UKIRT. *JHK* photometry was performed on 2007–05–27 and *LM* on 2007–06–19.

Object	Bandpass	Integration time (s)	Mean airmass	Magnitude
NGC 6834(1)	<i>J</i>	135	1.05	11.923±0.012
	<i>H</i>	90	1.05	11.685±0.018
	<i>K</i>	90	1.06	11.482±0.015
	<i>L'</i>	80	1.06	10.98±0.08
	<i>M'</i>	307.2	1.07	11.16±0.48
NGC 6834(2)	<i>J</i>	90	1.07	10.960±0.012
	<i>H</i>	45	1.06	10.697±0.018
	<i>K</i>	45	1.07	10.408±0.015
	<i>L'</i>	32	1.08	9.80±0.04
	<i>M'</i>	153.6	1.09	9.96±0.24

the observation log). The UKIRT faint standard FS 149 (Leggett et al. 2006) was observed using the 512×512 sub-array, dithering the star to five positions on the array, each with a separation of $10''$. The target fields were observed using the $1 \text{ k} \times 1 \text{ k}$ full array. A 9-point dither pattern with offsets of $20''$ from the central position was adopted for the target observations. A single frame with UFTI gives a field of view of $93'' \times 93''$ on the sky at a plate scale of $0.091'' \text{ pixel}^{-1}$. With a $20''$ dither pattern, the final mosaic has a field of view of $2.2' \times 2.2'$. A standard star was observed just before the target, at an airmass very close to that of the target. Hence, the extinction corrections are far less than the observational errors.

Two separate sets of target observations were obtained, each around NGC 6834(1) and NGC 6834(2), respectively. Dark frames were obtained before each set of target observations and they were subtracted from the object frames. Flat fielding was done using a flat field frame generated by median combining the dithered object frames. The magnitudes of the Be stars were estimated through the standard reduction procedure in IRAF, and the values are listed in Table 2.

Astrometric corrections were applied to our mosaics using the 2MASS positions as reference. 2MASS positions of typically nine isolated point sources were compared with the positions of these sources in our mosaics and the required coordinate offsets were applied. The J2000 coordinates (RA, Dec) derived for NGC 6834(1) and NGC 6834(2) are (19:52:06.471, +29:24:37.70) and (19:52:09.528, +29:23:34.14), respectively.

2.2.2 *L'M'* photometry

The *L'* and *M'* observations were performed with the UKIRT $1 - 5 \mu\text{m}$ imager spectrometer (UIST; Ramsay Howat et al. 2004) in photometric sky conditions. The $0.12'' \text{ pixel}^{-1}$ camera of UIST was used. For *L'* observations, a $1 \text{ k} \times 1 \text{ k}$ full array was used, whereas a 512×512 sub-array was used for *M'*. The object was dithered to four positions on the array for *L'*, and to eight positions on the array for *M'*. To counter the large sky background, individual pairs within these 4- or 8-point jitters were

subtracted from each other and flat fielded with flat fields generated by median combining the on-sky frames. These were then combined to form the final mosaics, which cover a field of $1.95' \times 1.65'$ in L' and $1.1' \times 1.2'$ in M' . The photometric standards GL811.1 and GL748 were observed in the L' and M' bands, respectively, at an airmass similar to that of the Be stars. Aperture photometry was performed using STARLINK GAIA; the derived magnitudes of the Be stars are given in Table 2.

2.2.3 WISE photometry

The Wide field Infrared Survey Explorer (*WISE*) carried out an all-sky survey from 3.4 to 22 μm with a sensitivity 100 times better than *IRAS*. The survey was done in four bands centered at 3.4, 4.6, 12 and 22 μm , which are labeled $W1$, $W2$, $W3$ and $W4$ respectively (Wright et al. 2010). The angular resolution in the four bands is $6.1''$, $6.4''$, $6.5''$, and $12''$ respectively. We queried for any detection of our targets in the *WISE* all-sky catalog through the IRSA database via the GATOR query engine. The search radius was fixed at $6''$, which is equivalent to the angular resolution in the first three *WISE* bands. *WISE* detected the sources in all four bands with definite errors and we have used these magnitudes for the present study.

2.3 Optical Spectroscopy

2.3.1 2.34-m Vainu Bappu Telescope

Medium resolution spectra were obtained using the Optomechanics Research (OMR) Spectrograph, mounted at the Cassegrain focus of the 2.34-m Vainu Bappu Telescope (VBT), Kavalur, India (Prabhu et al. 1998). The observations were performed with a 1200 l/mm grating, which provides an effective resolution of 4 \AA in the region of interest (around $H\alpha$ profile). FeNe lamp spectra were taken after the object for wavelength calibration. Dome flats were taken to correct the object frames for pixel-to-pixel efficiency. The extracted spectra were bias subtracted, flat-fielded and wavelength calibrated in the standard way using the software packages available in IRAF. The log of the observations is given in Table 3.

Table 3 Journal of Optical Spectroscopic Observations

Facility	Be star	Date	Integration time (s)	$H\alpha$ EW (\AA)	HeI 5876 EW (\AA)	HeI 6678 EW (\AA)
VBT	NGC 6834(1)	2007-11-14	2700	-37.3	-	-
	NGC 6834(2)	2007-11-15	2700	-34.7	-	0.17
HCT	NGC 6834(1)	2005-10-07	900	-38.9	0.58	0.36
		2007-07-05	900	-37.5	0.52	0.30
	NGC 6834(2)	2005-10-07	600	-42.5	0.32	0.24
		2007-07-06	600	-41.7	0.37	0.23

2.3.2 2-m Himalayan Chandra Telescope

The optical spectra of the Be stars in the wavelength range 5500–9000 \AA were obtained using the Himalayan Faint Object Spectrometer and Camera (HFOSC), mounted on the 2.1-m Himalayan Chandra Telescope (HCT). The spectra have a resolution of 7 \AA around the $H\alpha$ spectral region. The data reduction follows the method outlined in Mathew & Subramaniam (2011). The log of the observations is given in Table 3. We have two sets of spectra for each Be star - one before (2005–10–07) and another after (2007–07–06) the UKIRT observation. This allows us to check whether the source shows spectral variability in conjunction with the infrared spectra.

2.4 Optical Photometry

Optical photometry of NGC 6834 was performed on 2003–09–19 with HFOSC mounted on HCT. The cluster was observed in *UBV* with three different exposure times, (3 s, 10 s, 60 s) in *V*, (5 s, 60 s, 180 s) in *B* and (30 s, 180 s, 600 s) in *U*. These frames with variable exposures were needed to do the photometry of bright and faint cluster members. The nights were photometric, and the Landolt standards were observed for photometric calibrations. The zero point errors are 0.010, 0.013 and 0.018 mag in *V*, *B* and *U*, respectively. The data reduction and calibration procedure were the same as those elaborated in Subramaniam & Bhatt (2007). The magnitudes derived are given in Table 5.

3 RESULTS

3.1 Revised Estimates of Cluster Parameters from New Photometry

There is a scarcity of photometric data for this cluster, as seen from the WEBDA database (www.univie.ac.at/webda/).

Section 1 shows that a range of values is available for cluster parameters; hence, deep *UBV* CCD photometry which includes the faint stars is needed to better constrain these values. A precise estimation of age and distance for the cluster is important to constrain the evolutionary phase of the Be stars.

We obtained *UBV* CCD photometry of the cluster and re-estimated the cluster parameters. The *XY* plot of the cluster region is shown in Figure 2, with the Be stars and the evolved stars shown with separate symbols. A circle with a radius of $200''$, which is the cluster radius estimated from the radius density profile, is plotted in Figure 2. We derived a reddening value of $E(B - V) = 0.73$, which closely agrees with the earlier estimates by Moffat (1972) and Paunzen et al. (2006), who found values of 0.72 and 0.70, respectively. The distance modulus is estimated to be 14.8, from which a distance of 3100 pc is derived. This places the cluster at a higher distance than the previous estimates of 2750 pc by Miller et al. (1996) and 1930 pc by Paunzen et al. (2006). Moffat (1972) suggested that the limiting magnitude of the photometry should be low enough to include the faint stars, which are needed to do a better zero age main sequence fit to provide an accurate distance measurement. The superior nature of our photometry is relevant in this context because it revises the distance of NGC 6834 to 3100 pc. The age is estimated from the isochrones of Marigo et al. (2008), which indicates that most of the evolved candidates lie in the age range of 70–80 Myr. This new age measurement matches that of Moffat (1972), who found the cluster to be 80 Myr old.

We have identified four giants associated with the cluster, three within and one outside the cluster radius (see Fig. 2). Interestingly, one of these giants (shown as an asterisk in Fig. 2 that is located right beside a circled Be star) is identified as a companion to the Be star NGC 6834(1) from speckle interferometric studies (Mason et al. 2002). In addition, a yellow supergiant (YSG) is identified, which can be clearly distinguished in the color magnitude diagram (CMD). The YSG is near the blue loop, and is close to becoming a Cepheid. They were not found to be variables by Jerzykiewicz et al. (2011). The Be stars in the cluster are circled in Figure 2. Photometry is not available for NGC 6834(3), so it is not displayed.

The Be stars NGC 6834(1) and NGC 6834(2) are close to the evolved part of the main sequence (Fig. 3) and they have *V* magnitudes of 13.224 ± 0.006 and 12.518 ± 0.003 , respectively. Assuming a standard extinction law and using the revised cluster parameters ($E(B - V) = 0.73$, $d = 3100$ pc), the spectral types of NGC 6834(1) and NGC 6834(2) are estimated to be B3-5 and B2-3, respectively. Even though the Be stars are close to the evolved part of the main sequence, they are well separated from the giant star candidates identified in the cluster. Hence, we assume them to be main sequence stars. Estimates of their spectral types will be revisited in Section 3.3.

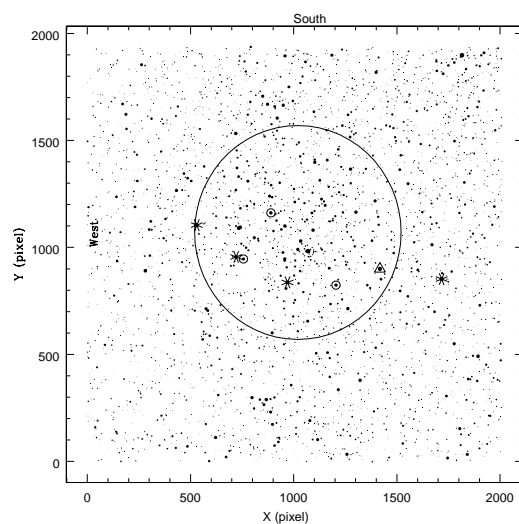


Fig. 2 X-Y plot of the cluster NGC 6834 is shown with the locations of the Be stars (encircled), giants (in asterisks) and YSG (in an open triangle) indicated.

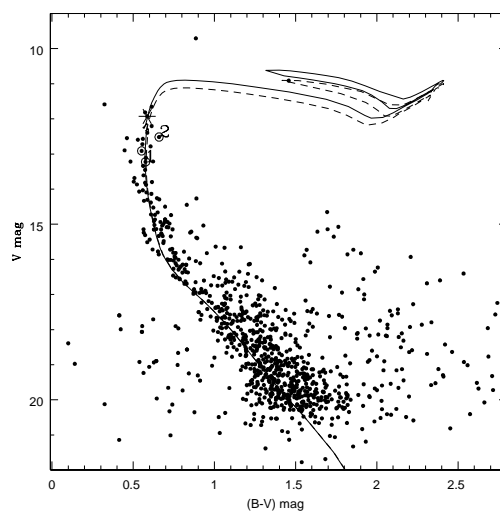


Fig. 3 The color-magnitude diagram of NGC 6834. The Be stars identified are circled; NGC 6834(1) and NGC 6834(2) are labeled as “1” and “2” respectively. The suspected binary companion to NGC 6834(1) is shown with an asterisk. The solid and dashed lines are the isochrones for ages 70 and 80 Myr, respectively.

3.2 Analysis of *JHK* Spectra

3.2.1 Description of *UKIRT JHK* spectra

Our *HK* spectra span a range of 1.5 – 2.5 μm , covering some of the prominent hydrogen recombination emission lines belonging to the Brackett and Pfund series. The spectra of the two Be stars are

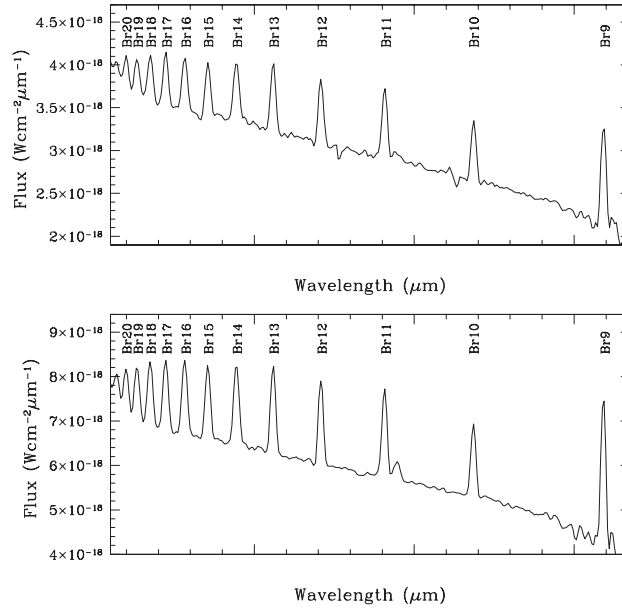


Fig. 4 Flux-calibrated H -band spectra of NGC 6834(1) and NGC 6834(2) are shown in the upper and lower panels respectively, with the prominent emission lines labeled.

shown separately for clarity and to avoid the region of poor atmospheric transmission. The spectra shown in Figure 4 cover the Brackett series from Br9 (1.8181 μm) to the series limit. The remaining emission lines belonging to the Brackett series (Br γ and Br8) and the higher order Pfund lines, from Pf17 to the series limit, are shown in Figure 5. The FeII 2.089 μm line is present in emission in the spectra of NGC 6834(2) (Fig. 5). Of the Be stars studied by Granada et al. (2010), only EW Lac showed an FeII 2.089- μm line in its spectra, which was identified as a characteristic of moderately warm and dense environments. The measured values of the EW and line flux of the Brackett and Pfund series emission lines in the spectra of each of the Be stars are shown in Table 4. The flux ratios of these lines are used to study the optical depth effects in Be stars, which is explained in the next section.

The spectra obtained using the short- J grism are shown in Figure 6. The signal-to-noise ratios of the spectra are quite low, so we have smoothed them for display purposes. Of the hydrogen recombination lines, only Pa γ (1.0938 μm) is visible in these spectra. Due to the small wavelength coverage of this grism, Pa β was not observed. The other interesting emission lines in the spectra are due to OI 1.1287 μm and FeII 1.050 μm , which are labeled in Figure 6. The spectra were not flux calibrated, so we will not be including these lines in further analysis. The presentation of these spectra highlights the absence of the HeI 1.083 μm emission line in both the Be stars, which can be corroborated with the HK spectra during the discussion on the spectral type of the Be stars.

3.2.2 Case B analysis of the hydrogen emission lines

From the conventional definition put forth by Baker & Menzel (1938), the Case B condition indicates that the Lyman lines are considered to be optically thick while all the other lines are assumed to be optically thin. Hummer & Storey (1987) estimated the emission strength of HI recombination lines under Case B conditions for a range of temperatures and densities (especially at higher densities, *viz.* $n_e > 10^{10} \text{ cm}^{-3}$) where the collision effects are important. In the case of Be stars, HI recombination

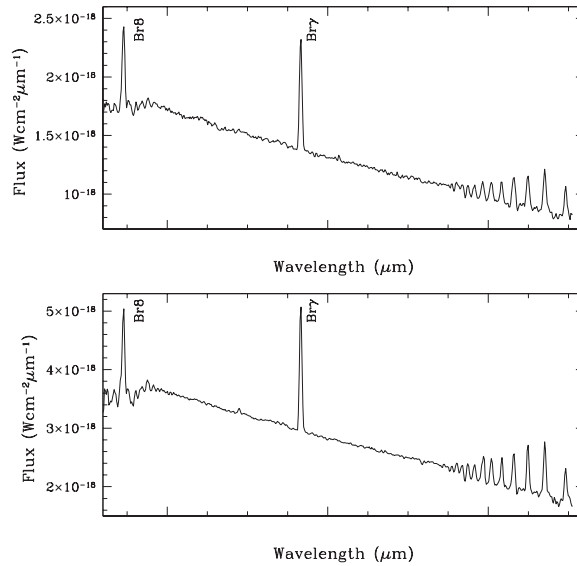


Fig. 5 Flux-calibrated K -band spectra of NGC 6834(1) and NGC 6834(2) are shown in the upper and lower panels respectively, with the prominent emission lines labeled.

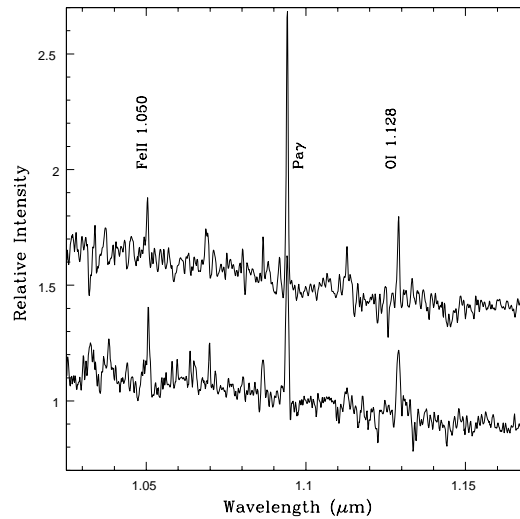


Fig. 6 The J -band spectra of NGC 6834(1) (*lower*) and NGC 6834(2) (*upper*) shown with a positive offset for clarity.

lines are formed in dense ($n_e = 10^{10} - 10^{14} \text{ cm}^{-3}$) regions of the circumstellar disk and, hence, we expect these lines to be optically thick (Ashok & Banerjee 2000; Steele & Clark 2001). Lenorzer et al. (2002) suggested using an $\text{Hu}14/\text{Br}\gamma$ versus $\text{Hu}14/\text{Pf}\gamma$ flux ratio diagram as the diagnostic to separate stars, which showed opacity effects from those for which H I emission strength followed Case B values. A similar method was followed by Granada et al. (2010), who identified the deviation

Table 4 EW and Line Flux Measurements from the Infrared Spectra

Line	λ (μm)	NGC 6834(1)		NGC 6834(2)	
		EW (\AA)	Line flux (Wm^{-2})	EW (\AA)	Line flux (Wm^{-2})
Pf17	2.4953	-12.3	9.967×10^{-18}	-11.7	2.081×10^{-17}
Pf18	2.4700	-17.7	1.523×10^{-17}	-15.4	2.963×10^{-17}
Pf19	2.4490	-12.1	1.084×10^{-17}	-13.8	2.676×10^{-17}
Pf20	2.4314	-13.9	1.238×10^{-17}	-11.9	2.350×10^{-17}
Pf21	2.4164	-7.3	6.831×10^{-18}	-8.3	1.678×10^{-17}
Pf22	2.4035	-7.9	7.517×10^{-18}	-8.3	1.703×10^{-17}
Pf23	2.3925	-7.1	6.762×10^{-18}	-8.9	1.867×10^{-17}
Pf24	2.3828	-4.5	4.380×10^{-18}	-4.6	9.872×10^{-18}
Pf25	2.3744	-3.9	3.808×10^{-18}	-4.3	9.155×10^{-18}
Br7	2.1661	-28.1	3.861×10^{-17}	-26.3	7.797×10^{-17}
Br8	1.9451	-15.7	2.730×10^{-17}	-14.5	5.251×10^{-17}
Br9	1.8181	-21.8	4.591×10^{-17}	-24.8	1.089×10^{-16}
Br10	1.7367	-10.2	2.688×10^{-17}	-11.6	6.174×10^{-17}
Br11	1.6811	-10.2	2.996×10^{-17}	-12.7	7.358×10^{-17}
Br12	1.6412	-10.0	3.057×10^{-17}	-11.7	7.083×10^{-17}
Br13	1.6114	-9.5	3.064×10^{-17}	-11.7	7.380×10^{-17}
Br14	1.5885	-7.9	2.697×10^{-17}	-10.7	6.999×10^{-17}
Br15	1.5705	-6.8	2.310×10^{-17}	-9.6	6.381×10^{-17}
Br16	1.5561	-6.8	2.387×10^{-17}	-10.1	6.778×10^{-17}
Br17	1.5443	-6.9	2.451×10^{-17}	-9.3	6.308×10^{-17}
Br18	1.5346	-5.3	1.910×10^{-17}	-7.7	5.340×10^{-17}

of the emission strength of HI emission lines belonging to Pfund and Humphrey series from optically thin Case B values. However, a comparison between the flux values of the HI recombination lines (obtained from the infrared spectra) with the theoretical estimates by Storey & Hummer (1995) will give a quantitative picture of the optical depth effects in Be stars. Mathew et al. (2012b) did this in the case of X Persei and found the observed flux values of the HI recombination lines belonging to Paschen and Brackett series to be higher than the theoretical values, thereby suggesting that these lines are optically thick. In this work, we extend the analysis to longer wavelengths, including the Pfund series of HI emission lines.

The flux calibrated spectra of the two Be stars are dereddened for a cluster with $E(B - V)$ of 0.73, using the task DEREDDEN in IRAF. The line flux values are measured for all the HI recombination lines belonging to the Brackett and Pfund series present in our spectra. The flux values of the Brackett lines Br8 (1.9451 μm) and Br9 (1.8181 μm) are susceptible to large errors because they are located in regions of poor atmospheric transmission. The flux ratios are calculated with respect to $\text{Br}\gamma$ and are shown in Figure 7. The Case B emissivity values corresponding to $T_e = 10^4$ K and $n_e = 10^{10}$, 10^{12} and 10^{14} cm^{-3} are obtained from Storey & Hummer (1995), and are shown using continuous lines in Figure 7. We have assumed the disk to be isothermal with a mean temperature of 10^4 K. The range of density values used for this study represents typical values of density prevailing in Be star disks (e.g. Waters 1986; Silaj et al. 2010). The observed flux ratios of all the HI lines belonging to Brackett and the Pfund series ($\text{Br}\gamma - \text{Br}18$ and $\text{Pf}17 - \text{Pf}25$) with respect to $\text{Br}\gamma$ are higher than the theoretical estimates, which implies that these lines are optically thick.

3.3 Re-estimation of the Spectral Type of the Be Stars

There is ambiguity about the accuracy of spectral types of Be stars. Even the spectral types of well-studied field Be stars from the catalog of Jaschek & Egret (1982) have been re-estimated a number of times using spectra with better sensitivity and resolution because the photospheric line and

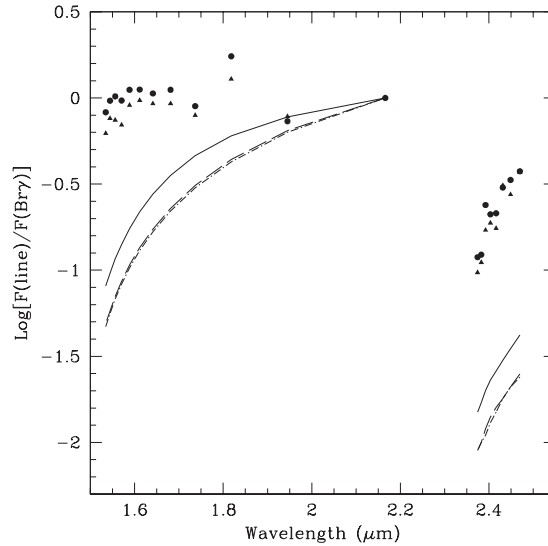


Fig. 7 Case B recombination analysis of the Brackett and Pfund series lines of hydrogen for NGC 6834(1) and NGC 6834(2). The line fluxes are normalized with respect to that of $\text{Br}\gamma$. The lines shown are Brackett 18 – Pfund 25 (1.5346 – 2.3744 μm). The flux values for NGC 6834(1) and NGC 6834(2) are shown in filled triangles and filled circles, respectively. The recombination analysis is carried out for $T_e = 10^4$ K. The continuous, dashed and dot-dashed lines show the Case B values for $n_e = 10^{10}$, 10^{12} and 10^{14} cm^{-3} respectively.

continuum emission can get modified by the emission from the circumstellar disk. From the revised *UBV* CCD photometry, we have estimated the spectral types of NGC 6834(1) and NGC 6834(2) to be B3-5V and B2-3V, respectively (as shown in Section 3.1). Classical Be stars are known to have circumstellar disks, which redden the stellar light, thereby biasing the estimates towards late spectral types (Slettebak 1982). A conventional way to estimate the spectral type from optical spectra is by matching the intensity of the prominent higher order H I (from H δ to H8) and He I absorption lines (4471, 4026, 4143 \AA) from a spectral library. The method is elaborated in Mathew & Subramaniam (2011). Adopting this technique we estimate spectral types as B5V and B1V for NGC 6834(1) and NGC 6834(2), respectively. The luminosity classification is consistent with the absence of the Mg II 4481 \AA absorption line in the spectra of both the Be stars, which are normally seen in the spectra of giants. However, there may still be pitfalls in the classification scheme since hydrogen and helium absorption lines can be filled-in by emission from the disk (even though we did a better job by using the lines least affected by contamination for classification). Hence, we consider an alternative scheme to do the spectral classification.

The present effort is to re-estimate the spectral types of NGC 6834(1) and NGC 6834(2) from the relative intensities of the emission lines in our 8300–8900 \AA optical spectra and near-infrared *JHK* spectra. We use the studies by Andrillat et al. (1988) and Clark & Steele (2000) as guidance for classification in this study.

3.3.1 From optical spectra

The 8300–8900 \AA optical spectra have been conventionally used to estimate the luminosity class of Be stars (e.g. Andrillat et al. 1988; Torrejon et al. 2010). The optical spectra of both Be stars in

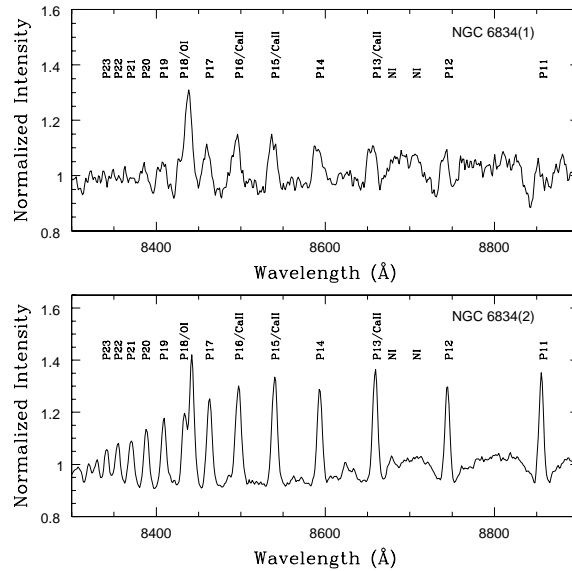


Fig. 8 The optical spectra of the Be stars NGC 6834(1) and NGC 6834(2) in the wavelength region 8300–8900 Å.

this wavelength regime are presented in Figure 8, and the prominent emission lines are labeled. The major emission lines are due to:

- (1) The neutral hydrogen lines belonging to the Paschen series – P11(8862), P12(8750), P13(8665), P14(8598), P15(8545), P16(8502), P17(8467), P18(8437), P19(8413), P20(8392), P21(8374), P22(8359), P23(8345);
- (2) CaII triplet – λ 8498, 8542, 8662;
- (3) OI λ 7772 Å (Multiplet M1; 7772-7774-7775; Moore 1945), 8446 Å (Multiplet M4; Moore 1945);
- (4) Ni composite λ 8686-8683-8680 and λ 8719-8712-8703;
- (5) FeII λ 7712.

The inclusion of OI λ 7772 and FeII λ 7712 in Figure 8 will affect the clarity of lines in the Paschen series, so they are not shown.

All the Paschen lines are present in the emissions from both stars, with the lines being more intense in NGC 6834(2) when compared to those in NGC 6834(1). The Paschen lines P13, P15 and P16 are stronger than the other lines in the series, which shows that they are blended with the CaII triplet. OI λ 7772 and λ 8446 are seen in emission in both the stars. FeII λ 7712 is present in emission in NGC 6834(2) whereas the emission is quite faint in NGC 6834(1). The lower order Paschen lines, especially P11 and P12, are embedded in the broad stellar absorption profile. Another notable point is the presence of the whole Paschen series of emission lines, down to the series limit, in the case of NGC 6834(2) but the series is more or less truncated by P20 in NGC 6834(1).

The presence of Paschen emission lines suggests that these Be stars have spectral types earlier than B3 since these lines show either fill-in features or absorption for later spectral types (Andrillat et al. 1988). Furthermore, the CaII triplet and FeII λ 7712 lines are present in emission in Be stars earlier than B2.5 (Andrillat et al. 1988). However, it is better to measure the EWs and full-width at half maximum (FWHM) of these stars, and then compare them with the template spectra given by Andrillat et al. (1988). The spectra of NGC 6834(1) closely resemble that of the B0.5IV Be star

HD 5394 in terms of the EWs of the Paschen lines and the truncation of the Paschen series at P20. The EW values of the Paschen lines of NGC 6834(2) agree with those of the Be star HD 148184 (for example, $EW(P14) \sim 2.8$), which is reported to be a B1.5Ve star. These new spectral types based on the strength of emission lines have to be contrasted with the earlier estimates, based on the strength of HeI and H α absorption lines. There is little difference between the spectral type of NGC 6834(2) estimated from both methods - B1 from the absorption lines, and B1.5 from the emission lines. However, NGC 6834(1) has been modified to an early-type star (B0.5) whereas the earlier estimates indicated it is a B5. From a visual examination (spectra not shown here), the hydrogen absorption lines from H γ to H8 seem to be intense in NGC 6834(1) (when compared to NGC 6834(2)) whereas HeI 4471, 4026, 4143 Å lines are intense in NGC 6834(2). Hence, NGC 6834(1) should be a later spectral type when compared with NGC 6834(2), which also agrees with the spectral estimates from photometry. This suggests that a classification scheme based on Paschen emission lines is only suggestive when the optical spectra in the visual region are not available or when the hydrogen and helium absorption lines are veiled, particularly in the case of pre-main sequence stars (Mathew et al. 2012a). Hence, at this point, NGC 6834(1) stands as a B5V star while NGC 6834(2) is modified to B1-B1.5V. The next step is to see if the estimates agree with the emission lines seen in the infrared spectra.

3.3.2 From infrared spectra

Clark & Steele (2000) introduced a spectral classification scheme in the infrared, wherein the Be stars are classified into five groups based on the presence and the relative strength of Br γ , HeI and MgII features in the *K*-band spectra. This is particularly useful in the spectral classification of highly-reddened counterparts of X-ray transient systems, which are subjected to large extinction in the optical.

Our sample of Be stars belongs to Group 5 of Clark & Steele (2000) by virtue of the presence of Br γ emission and the absence of HeI 1.083 μ m, 2.058 μ m and MgII 2.138/2.144 μ m spectral features (Fig. 5 & 6). Furthermore, Clark & Steele (2000) found that Group 5 Be stars belong to B5 or later spectral types. Br γ emission lines are intense in our sample of Be stars, with the EW values of NGC 6834(1) and NGC 6834(2) being 28 and 26 Å respectively. Interestingly, the strong emission in Br γ is not seen in any of the Be stars presented in Clark & Steele (2000).

This opens up a new riddle. For NGC 6834(1), the optical and infrared data suggest a B5 spectral type. However, NGC 6834(2) has been identified to be later than B5 from the infrared classification scheme, whereas we derive a spectral type of B1-1.5 from the optical spectra. NGC 6834(2) has been reported to be a variable (Jerzykiewicz et al. 2011). It can be seen from Table 3 that lines from HeI 6678 Å show variability between two epochs of observations. Therefore, we cannot rule out the possibility of a varying HeI 2.058 μ m profile in NGC 6834(2). The possibility of a companion influencing the spectral line features should also be considered since NGC 6834(2) has been suggested as a γ Cas-like variable. For the present purpose, we conclude the spectral type of Be stars NGC 6834(1) and NGC 6834(2) to be B5V and B1-1.5V, respectively.

We would like to point out the uncertainty of a classification scheme based on emission lines since the region of line formation in the disk is highly active, thereby inducing variability in spectral lines. In addition, the group classification scheme of Clark & Steele (2000) needs a revision by including a larger sample of Be stars since we found that the Br γ emission lines in NGC 6834(1) and NGC 6834(2) are more intense than any of the stars discussed in Clark & Steele (2000).

3.4 Spectral Energy Distribution

The SEDs of NGC 6834(1) and NGC 6834(2) are constructed using the new observations in the *B*, *V*, *J*, *H*, *K*, *L'* and *M'* bands presented in this work (Tables 5 and 2 respectively), and the *WISE* data

Table 5 Available magnitudes and colors of the candidate Be stars. Also given are the magnitudes of NGC 6834(1B), which is the proposed companion of the Be star NGC 6834(1).

Reference	Band	NGC 6834(1)	NGC 6834(2)	NGC 6834(1B)
This work	<i>V</i>	13.224±0.006	12.518±0.003	11.929±0.005
	<i>(B - V)</i>	0.576±0.006	0.659±0.003	0.586±0.010
HMUBV	<i>V</i>	13.20	–	–
	<i>(B - V)</i>	0.59	–	–
	<i>(U - B)</i>	-0.15	–	–
P06	<i>V</i>	13.22	12.47	11.95
	<i>(B - V)</i>	0.666	0.797	0.693
H61	<i>V</i>	13.210	–	11.940
	<i>(B - V)</i>	0.590	–	0.610
	<i>(U - B)</i>	-0.150	–	0.040
JKP11	<i>V</i>	13.117	12.463	–
	<i>(V - I_C)</i>	0.841	0.950	–
KW97	<i>V</i>	13.20	10.70	–
E92	<i>V</i>	–	11.90	–
Z04	<i>V</i>	–	12.140	–
F83	<i>P</i>	–	12.6	–
L96	<i>P</i>	–	11.46±0.40	–
K99	<i>B</i>	–	12.33	–
U98	<i>B</i>	–	13.05	–
UKIDSS	<i>J</i>	11.872±0.001	10.977	10.753
	<i>H</i>	11.737±0.001	10.942	10.906
	<i>K</i>	11.498±0.001	10.451±0.001	10.456
2MASS	<i>J</i>	11.796	10.868±0.021	10.602±0.021
	<i>H</i>	11.579±0.030	10.588±0.016	10.433±0.018
	<i>K</i>	11.223	10.392±0.018	10.400±0.018
WISE	<i>W1</i>	10.741±0.024	9.919±0.022	10.263±0.025
	<i>W2</i>	10.541±0.021	9.699±0.020	10.307±0.023
	<i>W3</i>	10.030±0.067	8.927±0.037	10.327±0.106
	<i>W4</i>	8.558±0.285	7.617±0.124	8.964

References: KW97 – Kohoutek & Wehmeyer (1997), JKP11 – Jerzykiewicz et al. (2011), HMUBV – Homogeneous Means in the UBV System (Mermilliod 1997), P06 – Paunzen et al. (2006), H61 – Hoag et al. (1961), F83 – Fresneau (1983), L96 – Lasker et al. (1996), K99 – Kislyuk et al. (1999), U98 – Lucas et al. (2008), E92 – Egret et al. (1992), Z04 – Zacharias et al. (2004), *UKIDSS* –, 2MASS – Cutri et al. 2003, *WISE* – Cutri et al. 2012

in the four bands *W1*, *W2*, *W3* and *W4* given in Table 5. The magnitudes are extinction corrected for $E(B - V) = 0.73$, using the relations in Rieke & Lebofsky (1985). The extinction corrected *BVJHKL'M'* magnitudes are converted to flux using the zero-magnitude flux values from Bessell et al. (1998) and the JAC/UKIRT homepage¹. The *WISE* magnitudes are corrected for extinction and converted to flux using the zero-magnitude flux values given in the *WISE* explanatory supplement (Jarrett et al. 2011).

The SEDs of the Be stars NGC 6834(1) and NGC 6834(2) are shown in Figure 9. The blackbody curves are generated corresponding to the effective temperature of the stars, using the values tabulated in Schmidt-Kaler (1982) for different spectral types, and adopting B5V for NGC 6834(1) and B1-1.5V for NGC 6834(2). The blackbody curves are normalized to the extinction corrected *V* band flux values of the two stars. It can be seen from Figure 9 that the blackbody curves poorly fit the SEDs in the infrared region, thereby indicating the presence of IR excess in these stars. It has been demonstrated from various studies that IR excess in Be stars is due to free-free emission from free electrons in the disk (Gehrz et al. 1974). In Mathew et al. (2012b), we used a simplified model to examine if the free-free emission can account for the IR excess in the Be star X Persei. In this work

¹ http://www.jach.hawaii.edu/UKIRT/astrometry/calib/phot_cal/conver.html

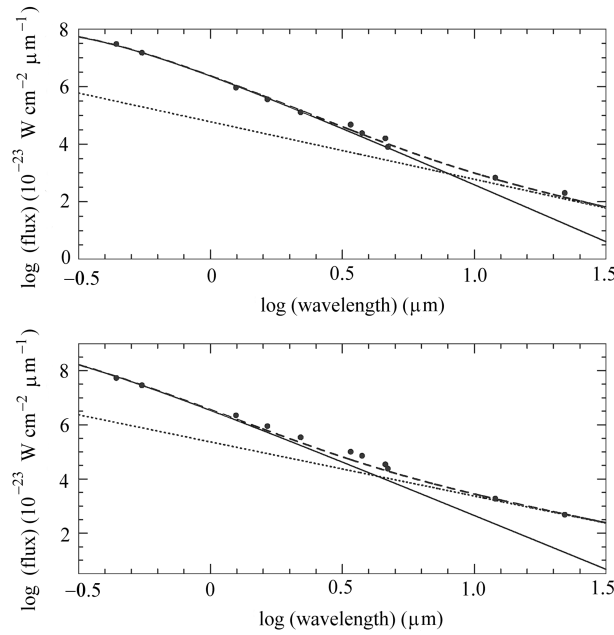


Fig. 9 SEDs of NGC 6834(1) and NGC 6834(2). The dotted lines show the contribution from the free-free emission, calculated as a function of wavelength. The solid lines show the blackbody emission for temperatures appropriate for the spectral types of the two stars. The dashed lines show the total contributions from the blackbody and the free-free components.

we use the same method to model the excess flux seen in Figure 9. The input parameters needed for the model are the temperature, electron density, stellar radius and the distance to the Be star. The radii of the Be stars corresponding to their spectral types are taken from Gehrz et al. (1974). The cluster distance of 3100 pc is used. The electron density is a free parameter, whose value is optimized from the fit to the data points. The calculated flux values of free-free emission as a function of wavelength are shown by a dotted line in Figure 9. These flux values are calculated for a temperature of 10 000 K. We derive electron densities (n_e) of $2 \times 10^{11} \text{ cm}^{-3}$ for NGC 6834(1), and $1.5 \times 10^{11} \text{ cm}^{-3}$ for NGC 6834(2). These values of electron density agree with the values derived from theoretical modeling by Silaj et al. (2010) for Be stars of similar spectral types.

4 DISCUSSION

4.1 On the Binarity of NGC 6834 (1)

Mason et al. (2002), from speckle interferometric studies, suggested a possible companion to NGC 6834(1) at a separation of $10.35''$ and a position angle of 74.7° . The system is designated by Washington Speckle Interferometry (WSI) number WSI 12. They derived the V magnitudes of the primary and secondary as 11.7 and 12.1, respectively. The epoch of the observation was 2001.738 (given as fractional Besselian year). The measurements of the WSI 12 system were repeated after two years (Epoch = 2003.782) and the results are presented in Mason et al. (2004). The separation of the components and the position angle are $10.96''$ and 74.4° , respectively. The results from the second observations agree with the previous estimates.

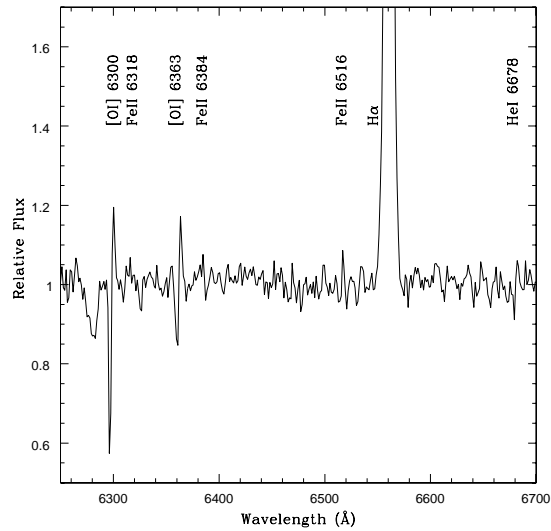


Fig. 10 Optical spectra (6250–6700 Å) of NGC 6834(1) observed on 2007-11-14 using the OMR spectrograph mounted on VBT showing [O I] 6300, 6363 Å emission lines.

In the POSS II *R*-band image (Fig. 1), the star immediately beside NGC 6834(1), located at RA = 19:52:05.70 and Dec = +29:24:36.4, is the possible companion reported by Mason et al. (2002). This is the only star at the distance of 10.35'' from the Be star. This star (denoted by NGC 6834(1B) in this work) has been identified as a B-type giant (B5III) by Turner (1976). NGC 6834(1B) also appeared in the photoelectric studies of Hoag et al. (1961) (numbered 7 while Be star is numbered 16), whose magnitudes and colors are given in Table 5. From our new optical photometry it can be seen that the *V* mag of the Be star is 13.22 while that of the proposed companion is 11.93. When compared to the Be star, the B-type giant is brighter by 1.3 mag in *V*, ~ 1 mag in *JHK* and 0.2–0.5 mag in the *WISE* bands. A tentative trend of reversal in brightness, with the Be star brighter than a B-type giant, is seen in the W3 and W4 bands. This is due to the fact that the IR excess from the disk of the Be star starts to dominate in this region (as shown in Fig. 9) whereas the blackbody emission from NGC 6834(1B) keeps decreasing.

It can be seen from Table 5 that most of the photometric measurements quote a *V* mag of 13.2 for NGC 6834(1) and 11.9 for NGC 6834(1B). If we compare these values with the speckle measurements, NGC 6834(1B) matches very well whereas the Be star was brighter by about 1 mag during speckle measurements. The *V* mag measurements by Jerzykiewicz et al. (2011) were also done during the same period (April–October 2001) and they report a value of 13.117 for the Be star. Paunzen et al. (2006) also obtained a similar value (*V* = 13.22) from their observations conducted in August 2004. This presents a puzzle regarding the brighter magnitude reported for the Be star in speckle interferometric observations. The only measurement reported in the literature which closely agrees with the value of Mason et al. (2002) is from the NOMAD Catalog (Zacharias et al. 2004), who reported a *V* mag of 12.390. This is a compilation of various observations done in the US Naval Observatory and this particular measurement was taken from the YB6 Catalog (USNO, unpublished). This difference between the magnitudes of the Be star from photometry and speckle interferometry (both of which are obtained during the same period) hinders the discussion on the nature of the binary system. In the future we may try to get radial velocity measurements of both stars to look for a possible association between them.

Another interesting observation worth reporting is the detection of the [OI] 6300 and 6363 Å emission lines in the spectra of NGC 6834(1), obtained at a resolution of 4 Å from the 2.34-m VBT, Kavalur (Fig. 10). The [OI] 6300, 6363 Å lines show a P-Cygni feature, which is indicative of the mass-loss process in the Be star (Fig. 10). If the lines are formed in the outflow, the outflow velocity can be calculated from the difference between the absorption and emission components of [OI] lines. The estimated value of 124 km s^{-1} (for both the lines) closely matches the values estimated for young stellar objects (YSOs; Acke et al. 2005). The chance of NGC 6834(1) being a YSO is feeble since such a pre-main sequence star is generally not found in an 80 Myr old cluster. In addition, from the optical CMD (Fig. 3) we found that the star is close to the evolved part of the main sequence. There are no reported cases of the presence of [OI] lines (especially with P-Cygni nature) in classical Be stars and the significance of this intriguing observation needs to be better understood.

Since NGC 6834 (1B) is separated from the Be star by $10.35''$, the chance of the giant influencing the Be star is minimal. In addition, the reason for outflow (deduced from [OI] lines) in NGC 6834(1) needs to be analyzed from a fresh set of observations. The role of a hidden companion triggering this outflow has to be explored even though we do not identify any high energy emission associated with the system.

4.2 NGC 6834 (2) - a γ Cas-like Variable?

γ Cas displays moderately high X-ray luminosity ($10^{32} - 10^{33} \text{ erg s}^{-1}$), which is an order of magnitude higher than that seen in massive stars of a similar spectral type. In addition, the X-ray emission is characterized by a hot thermal component of $T \sim 140-165 \text{ MK}$ whereas the plasma temperature for soft X-ray emission in other massive stars is identified to be 6 MK (Lopes de Oliveira & Motch 2011). The X-ray spectrum of γ Cas is similar to that of cataclysmic variables, which supports the idea that accretion onto the white dwarf is responsible for the high energy emission. Alternatively, the high energy component in X-ray emission can also be due to the magnetic reconnection at the interface between the photosphere and the inner part of the disk (Smith & Robinson 2003). γ Cas-like variables are Be stars that are characterized by an unusually hard thermal X-ray spectrum, variable on short time scales, and an early B-type optical spectrum with a dense circumstellar disk.

Jerzykiewicz et al. (2011) found that NGC 6834(2) exhibits short-term variability in V and I_C bands, with amplitudes of 0.23 and 0.22 mag respectively. This variability in optical bands along with the strong $H\alpha$ emission prompted Jerzykiewicz et al. (2011) to include NGC 6834(2) in the class of γ Cas-like variables. However, they have not mentioned any X-ray studies of this object.

γ Cas-like variables are characterized in the optical and infrared by means of the variability in their light curves, strong $H\alpha$ emission and IR excess. The strong $H\alpha$ emission along with the infrared excess is indicative of a dense circumstellar disk (Lopes de Oliveira & Motch 2011). Excess emission in the near- and mid-infrared region is clearly evident in the SED of NGC 6834(2) (Fig. 9). A strong $H\alpha$ emission ($EW = 42 \text{ \AA}$) is noticed in NGC 6834(2), which is found to be variable, fading by 7 \AA over a period of four months (see Table 3). From the archival data we found that NGC 6834(2) showed long-term variability of 0.7–1.1 mag in V (see Table 5). Kohoutek & Wehmeyer (1997) reported the star to be brighter by 1.7 mag in the V -band ($V = 10.7$), which is indicative of flaring activity during that period. In addition, Jerzykiewicz et al. (2011) identified short-term variability of 0.2 mag. Hence, this fulfills the criteria required in optical and infrared for the Be star to belong to the class of γ Cas-like variables. However, in addition to the above requirements, moderately high X-ray emission is a necessary criterion to classify the object as a γ Cas-like variable. Since we have not found any reports of X-ray (or high energy) emissions from this object, we are not certain about the classification.

Acknowledgements We thank the anonymous reviewer for helpful comments. The UKIRT is operated by the Joint Astronomy Centre on behalf of the Science and Technology Facilities Council (STFC) of the UK. We thank the UKIRT service program for obtaining the IR observations. We

would like to thank the support astronomers in HCT and VBT. The research work at the Physical Research Laboratory is funded by the Department of Space, Government of India. This research has made use of the VizieR catalogue access tool, CDS, Strasbourg, France. The original description of the VizieR service was published in A&AS 143, 23.

References

- Acke, B., van den Ancker, M. E., & Dullemond, C. P. 2005, A&A, 436, 209
- Andrillat, Y., Jaschek, M., & Jaschek, C. 1988, A&AS, 72, 129
- Ashok, N. M., & Banerjee, D. P. K. 2000, in IAU Colloq. 175: The Be Phenomenon in Early-Type Stars, Astronomical Society of the Pacific Conference Series, 214, eds. M. A. Smith, H. F. Henrichs, & J. Fabregat (San Francisco, CA: ASP), 468
- Ashok, N. M., Bhatt, H. C., Kulkarni, P. V., & Joshi, S. C. 1984, MNRAS, 211, 471
- Baker, J. G., Menzel, D. H., 1938, ApJ, 88, 52
- Banerjee, D. P. K., Janardhan, P., & Ashok, N. M. 2001, A&A, 380, L13
- Bessell, M. S., Castelli, F., & Plez, B. 1998, A&A, 333, 231
- Clark, J. S., & Steele, I. A. 2000, A&AS, 141, 65
- Collins, G. W., II 1987, in IAU Colloq. 92: Physics of Be Stars, eds. A. Slettebak & T. P. Snow (Cambridge: Cambridge Univ. Press), 3
- Cutri, R. M., et al., 2012, VizieR Online Data Catalog, 2311, 0
- Cutri, R. M., Skrutskie, M. F., van Dyk, S., et al. 2003, 2MASS All Sky Catalog of Point Sources, NASA/IPAC Infrared Science Archive
- Dougherty, S. M., Waters, L. B. F. M., Burki, G., et al. 1994, A&A, 290, 609
- Egret, D., Didelon, P., McLean, B. J., Russell, J. L., & Turon, C. 1992, A&A, 258, 217
- Fresneau, A. 1983, AJ, 88, 1378
- Fünfschilling, H. 1967, ZAp, 66, 440
- Gehrz, R. D., Hackwell, J. A., & Jones, T. W. 1974, ApJ, 191, 675
- Granada, A., Arias, M. L., & Cidale, L. S. 2010, AJ, 139, 1983
- Hoag, A. A., Johnson, H. L., Iriarte, B., et al. 1961, Publ. US Naval Obs., 2d Ser., 17 (Washington: US Naval Obs.), 347
- Jarrett, T. H., Cohen, M., Masci, F., et al. 2011, ApJ, 735, 112
- Hummer, D. G., & Storey, P. J. 1987, MNRAS, 224, 801
- Jaschek, M., & Egret, D. 1982, in IAU Symposium, 98, Be Stars, eds. M. Jaschek, & H.-G. Groth, 261
- Jerzykiewicz, M., Kopacki, G., Pigulski, A., Kołaczowski, Z., & Kim, S.-L. 2011, Acta Astronomica, 61, 247
- Kislyuk, V., Yatsenko, A., Ivanov, G., Pakulyak, L., & Sergeeva, T. 1999, in The FON astrographic catalogue (FONAC), Main Astronomical Observatory of National Academy of Science of Ukraine
- Kohoutek, L., & Wehmeyer, R. 1997, Catalogue of stars in the northern Milky Way having H-alpha in emission (Hamburg: Sternwarte)
- Leggett, S. K., Currie, M. J., Varricatt, W. P., et al. 2006, MNRAS, 373, 781
- Lasker, B. M., Sturch, C. R., Lopez, C., et al. 1996, VizieR Online Data Catalog, 2143, 0
- Lenorzer, A., de Koter, A., & Waters, L. B. F. M. 2002, A&A, 386, L5
- Lucas, P. W.; Hoare, M. G.; Longmore, A. et al. 2008, MNRAS, 391, 136
- Lopes de Oliveira, R., & Motch, C. 2011, ApJ, 731, L6
- Marigo, P., Girardi, L., Bressan, A. et al. 2008, A&A, 482, 883
- Mason, B. D., Hartkopf, W. I., Urban, S. E., et al. 2002, AJ, 124, 2254
- Mason, B. D., Hartkopf, W. I., Wycoff, G. L., et al. 2004, AJ, 128, 3012
- Mathew, B., Subramaniam, A., & Bhatt, B. C. 2008, MNRAS, 388, 1879
- Mathew, B., & Subramaniam, A. 2011, Bulletin of the Astronomical Society of India, 39, 517

- Mathew, B., Banerjee, D. P. K., Ashok, N. M., et al. 2012a, RAA (Research in Astronomy and Astrophysics), 12, 167
- Mathew, B., Banerjee, D. P. K., Naik, S., & Ashok, N. M. 2012b, MNRAS, 423, 2486
- Mermilliod, J. C. 1997, VizieR Online Data Catalog, 2168, 0
- Miller, G. J., Grebel, E. K., & Yoss, K. M. 1996, Bulletin of the American Astronomical Society, 28, 1367
- Moffat, A. F. J. 1972, A&AS, 7, 355
- Moore, C. E. 1945, Contributions from the Princeton University Observatory, 20, 1
- Paunzen, E., Netopil, M., Iliev, I. K., et al. 2006, A&A, 454, 171
- Porter, J. M., & Rivinius, T. 2003, PASP, 115, 1153
- Prabhu, T. P., Anupama, G. C., Surendiranath, R., 1998, BASI, 26, 383
- Ramsay Howat, S. K., Todd, S., Leggett, S., et al. 2004, In Proc Spie 5492, UV and Gamma-Ray Space Telescope Systems, eds. Hasinger, G., & Turner, M. J. 1160
- Rayner, J. T., Cushing, M. C., & Vacca, W. D. 2009, ApJS, 185, 289
- Rieke, G. H., & Lebofsky, M. J. 1985, ApJ, 288, 618
- Rivinius, T., Carciofi, A. C., & Martayan, C. 2013, A&A Rev., 21, 69
- Roche, P. F., Lucas, P. W., Mackay, C. D., et al. 2003, in Society of Photo-Optical Instrumentation Engineers (SPIE) Conference Series, 4841, Instrument Design and Performance for Optical/Infrared Ground-based Telescopes, eds. M. Iye, & A. F. M. Moorwood, 901
- Ruprecht, J. 1966, Bulletin of the Astronomical Institutes of Czechoslovakia, 17, 33
- Schmidt-Kaler, T. 1982, Landolt-Börnstein: Numerical Data and Functional Relationships in Science and Technology, eds. K. Schaifers, & H. Voigt (Berlin: Springer), VI/2b
- Silaj, J., Jones, C. E., Tycner, C., Sigut, T. A. A., & Smith, A. D. 2010, ApJS, 187, 228
- Slettebak, A. 1982, ApJS, 50, 55
- Slettebak, A. 1988, PASP, 100, 770
- Smith, M. A., & Robinson, R. D. 2003, in Astronomical Society of the Pacific Conference Series, 292, Interplay of Periodic, Cyclic and Stochastic Variability in Selected Areas of the H-R Diagram, ed. C. Sterken, 263
- Steele, I. A., & Clark, J. S. 2001, A&A, 371, 643
- Storey, P. J., & Hummer, D. G. 1995, MNRAS, 272, 41
- Subramaniam, A., & Bhatt, B. C. 2007, MNRAS, 377, 829
- Torrejón, J. M., Negueruela, I., Smith, D. M., Harrison, T. E., 2010, A&A, 510, A61
- Townsend, R. H. D., Owocki, S. P., & Howarth, I. D. 2004, MNRAS, 350, 189
- Trumpler, R. J. 1930, Lick Observatory Bulletin, 14, 154
- Turner, D. G. 1976, AJ, 81, 1125
- Urban, S. E., Corbin, T. E., Wycoff, G. L., et al. 1998, AJ, 115, 1212
- Wright, E. L., Eisenhardt, P. R. M., Mainzer, A. K. et al. 2010, AJ, 140, 1868
- Zacharias, N., Monet, D. G., Levine, S. E., et al. 2004, Bulletin of the American Astronomical Society, 36, 1418